Journal of Low Temperature Physics (2023) 212:113–126
https://doi.org/10.1007/s10909-023-02981-3

Boundary Effect and Critical Temperature of Two-Band Superconducting Films: Application to MgB_2

Jia-Hui Chen[1] · Jian-Tao Che[1] · Chen-Xiao Ye[1] · Hai Huang[1]

Received: 11 March 2022 / Accepted: 19 May 2023 / Published online: 20 June 2023

Abstract
Based on the two-band Bogoliubov–de Gennes theory, we study the boundary effect of an interface between a two-gap superconductor and an insulator (or vacuum). New boundary terms are introduced into the two-band Ginzburg–Landau free energy, which modifies the boundary conditions for the corresponding order parameters of the superconductor. A microscopic analysis of these terms is also given and the characteristic length scale of the boundary effect can be estimated. The theory allows for a simple calculation of the critical temperature suppression with the decrease in film thickness for the typical two-band superconductor magnesium diboride. Our numerical results are in good agreement with the experimental data observed in this material.

Keywords Two-band superconductor · Boundary term · Critical temperature · Magnesium diboride

1 Introduction

Since the discovery of superconductivity at about 40 K in magnesium diboride [1], the exploration on the superconducting mechanism and physical properties of this compound has attracted much attention over the past decades. The MgB_2

✉ Hai Huang
huanghai@ncepu.edu.cn

Jia-Hui Chen
cjh@ncepu.edu.cn

Jian-Tao Che
chejt2013@ncepu.edu.cn

Chen-Xiao Ye
yechenxiao@ncepu.edu.cn

[1] Department of Mathematics and Physics, North China Electric Power University, Beijing 102206, China

crystal consists of hexagonal-close-packed layers of Mg atoms alternating with graphite-like honeycomb layers of B atoms. The electronic structure of MgB_2 is now rather well-known, and the superconductivity is ascribed to the conventional electron–phonon mechanism [2–5]. The Fermi surface of this compound consists of two three-dimensional sheets from the π band, and two nearly cylindrical sheets from the two-dimensional σ band. The qualitative difference between these two bands suggests a multi-band description of superconductivity [6, 7]. This two-gap picture has been clearly confirmed by de Haas-van Alphen quantum oscillation measurements, scanning tunneling microscopy, specific heat measurements and other experiments [8–12].

High-quality MgB_2 films are also important for both fundamental research and electronic, high-field and radio frequency cavity applications. Much effort has been devoted to the deposition of MgB_2 thin films, and tremendous progress has been achieved by various deposition techniques [13]. Of all these techniques, hybrid physical–chemical vapor deposition (HPCVD) has been the most effective one for MgB_2 [14, 15]. So far, a wide range of works by various groups using HPCVD films have been performed in the research of MgB_2. For example, a series of MgB_2 superconducting films with the thickness ranging from 8 μm to 8 nm have been fabricated on SiC substrates by this method [16, 17]. It was found that T_c stays around the bulk value for the MgB_2 film thicker than 300 nm, but it will be reduced by 13% when the film thickness decreases from 30 to 8 nm. Pan et al. have grown epitaxial MgB_2 films between 40 nm and 10 nm on MgO substrates and performed electrical transport measurements to study the thickness dependence of the superconducting critical temperature [18]. A dramatic depression of T_c has also been observed and the critical temperature reaches about 34 K in the 10-nm film. Different mechanisms have been proposed to account for this T_c suppression in MgB_2 thin films, such as quantum phase fluctuations of the superconducting pair wave function [19] or enhanced Coulomb interaction due to disorder [20]. But up to now, there is still no consensus on the explanation of the experimental data mentioned above.

In this paper, we propose that the T_c dependence on the film thickness is due to the influence of boundary effect between the two-band superconductor and the insulator (or vacuum). We first introduce the appropriate boundary conditions for the Ginzburg–Landau (GL)-order parameters at the superconductor–insulator interface. We then give a microscopic analysis of new boundary terms based on the two-band Bogoliubov–de Gennes theory and obtain the characteristic length scales of the boundary effect as 268 and 383 nm for MgB_2. We end up with the computation on the film thickness dependence of critical temperature based on the two-band GL theory and the tight-binding model. Our theoretical results are consistent with the experimental data of MgB_2 films, which suggests the boundary effect is an important factor for the understanding of superconducting properties in this compound.

The rest of this article is structured as follows. In Sect. 2, we review the two-band Bogoliubov–de Gennes theory and the GL equations and propose the boundary terms for the superconductor-insulator interface. In Sect. 3, we give a microscopic derivation of these boundary conditions based on the Bogoliubov–de Gennes formalism. In Sect. 4, we perform the calculation on the film thickness

dependence of critical temperature for the compound MgB_2 in the frame of the GL theory. In Sect. 5, we compute the critical temperature of MgB_2 films based on the tight-binding model. Section 6 is the conclusion of the paper.

2 Two-Band Ginzburg–Landau Theory and Boundary Conditions at Interface

Based on the work of Zhitomirsky and Dao [21], we write the Hamiltonian of a two-band superconductor as

$$H = \sum_{i\sigma} c^{\dagger}_{i\sigma}(\boldsymbol{r})\hat{h}(\boldsymbol{r})c_{i\sigma}(\boldsymbol{r}) - \sum_{ii'} g_{ii'}c^{\dagger}_{i\uparrow}(\boldsymbol{r})c^{\dagger}_{i\downarrow}(\boldsymbol{r})c_{i'\downarrow}(\boldsymbol{r})c_{i'\uparrow}(\boldsymbol{r}). \tag{1}$$

Here, $i, i' = 1, 2$ are the band indices and $\sigma = \uparrow, \downarrow$ is the spin index. $\hat{h}(\boldsymbol{r})$ is the single-particle Hamiltonian of the normal metal, and $g_{ii'}$ are the electron–phonon interaction constants with $g_{12} = g_{21}$.

We can introduce gap functions

$$\Delta_i(\boldsymbol{r}) = -\sum_{i'} g_{ii'}\langle c_{i'\downarrow}(\boldsymbol{r})c_{i'\uparrow}(\boldsymbol{r})\rangle \tag{2}$$

and transform the Hamiltonian into the mean field form

$$H_{\text{eff}} = \sum_{i\sigma} c^{\dagger}_{i\sigma}(\boldsymbol{r})\hat{h}(\boldsymbol{r})c_{i\sigma}(\boldsymbol{r}) + \sum_{i}[\Delta_i(\boldsymbol{r})c^{\dagger}_{i\uparrow}(\boldsymbol{r})c^{\dagger}_{i\downarrow}(\boldsymbol{r}) + \text{H.}c.]. \tag{3}$$

This effective Hamiltonian can be diagonalized by means of the Bogoliubov transformation with b and $b^{\dagger}$ the annihilation and creation operators of quasi-particle excitations

$$c_{i\uparrow}(\boldsymbol{r}) = \sum_{\boldsymbol{k}}[u_{i\boldsymbol{k}}(\boldsymbol{r})b_{i\boldsymbol{k}\uparrow} - v^{*}_{i\boldsymbol{k}}(\boldsymbol{r})b^{\dagger}_{i\boldsymbol{k}\downarrow}] \tag{4}$$

and

$$c_{i\downarrow}(\boldsymbol{r}) = \sum_{\boldsymbol{k}}[u_{i\boldsymbol{k}}(\boldsymbol{r})b_{i\boldsymbol{k}\downarrow} + v^{*}_{i\boldsymbol{k}}(\boldsymbol{r})b^{\dagger}_{i\boldsymbol{k}\uparrow}] \tag{5}$$

where $\boldsymbol{k}$ is the wave vector. With the anti-commutation relations between the fermion operators and the equation of motion for $c_{i\sigma}(\boldsymbol{r})$, we can obtain the Bogoliubov–de Gennes equations for a two-band superconductor [22–25]

$$\begin{pmatrix} \hat{h} & \Delta_i(\boldsymbol{r}) \\ \Delta^{*}_i(\boldsymbol{r}) & -\hat{h}^{*} \end{pmatrix}\begin{pmatrix} u_{i\boldsymbol{k}}(\boldsymbol{r}) \\ v_{i\boldsymbol{k}}(\boldsymbol{r}) \end{pmatrix} = E_{i\boldsymbol{k}}\begin{pmatrix} u_{i\boldsymbol{k}}(\boldsymbol{r}) \\ v_{i\boldsymbol{k}}(\boldsymbol{r}) \end{pmatrix} \tag{6}$$

where $E_{i\boldsymbol{k}}$ is the energy of the excitation. Then with Eq. (2), we can transform the self-consistent gap equations into

$$\Delta_i(\boldsymbol{r}) = \sum_{i'\boldsymbol{k}} g_{ii'} v^*_{i'\boldsymbol{k}}(\boldsymbol{r}) u_{i'\boldsymbol{k}}(\boldsymbol{r}) \times [1 - 2f(E_{i'\boldsymbol{k}})] \tag{7}$$

with $f(E_{i\boldsymbol{k}}) = [1 + \exp(E_{i\boldsymbol{k}}/k_B T)]^{-1}$.

In the analogy with the single-band case [26], for small gap functions Δ_i, we can obtain the linearized form of self-consistency conditions from Eqs. (6) and (7) as

$$\Delta_i(\boldsymbol{r}) = \sum_{i'} \int K_{ii'}(\boldsymbol{r}, \boldsymbol{r'}) \Delta_{i'}(\boldsymbol{r'}) \mathrm{d}\boldsymbol{r'} \tag{8}$$

with the kernel

$$\begin{aligned} K_{ii'}(\boldsymbol{r}, \boldsymbol{r'}) = \frac{g_{ii'}}{2} \sum_{\boldsymbol{k}\boldsymbol{k'}} \Bigg[& \frac{\tanh\left(\frac{\varepsilon_{i'\boldsymbol{k}}}{2k_B T}\right) + \tanh\left(\frac{\varepsilon_{i'\boldsymbol{k'}}}{2k_B T}\right)}{\varepsilon_{i'\boldsymbol{k}} + \varepsilon_{i'\boldsymbol{k'}}} \\ & \times \Phi^*_{i'\boldsymbol{k}}(\boldsymbol{r'}) \Phi^*_{i'\boldsymbol{k'}}(\boldsymbol{r'}) \Phi_{i'\boldsymbol{k}}(\boldsymbol{r}) \Phi_{i'\boldsymbol{k'}}(\boldsymbol{r}) \Bigg]. \end{aligned} \tag{9}$$

Here, $\Phi_{i'\boldsymbol{k}}(\boldsymbol{r})$ is defined as the normal-state eigenfunction of the electron, $\hat{h}\Phi_{i'\boldsymbol{k}} = \varepsilon_{i'\boldsymbol{k}}\Phi_{i'\boldsymbol{k}}$.

With the explicit expressions of the kernels in the bulk system and the addition of nonlinear terms to the gap equations, we can obtain the two-band GL equations from Eq. (8) as [21]

$$\alpha_1(T)\Delta_1 + \beta_1|\Delta_1|^2\Delta_1 - \gamma_1(\nabla - \mathrm{i}\boldsymbol{A})^2\Delta_1 - R_{12}\Delta_2 = 0 \tag{10}$$

and

$$\alpha_2(T)\Delta_2 + \beta_2|\Delta_2|^2\Delta_2 - \gamma_2(\nabla - \mathrm{i}\boldsymbol{A})^2\Delta_2 - R_{12}\Delta_1 = 0 \tag{11}$$

with the GL parameters

$$\alpha_{1,2} = N_{1,2}\left[\frac{\lambda_{22,11}}{\lambda} - \frac{1}{\lambda_{\max}} - \ln\left(\frac{T_{c0}}{T}\right)\right], \quad \beta_i = \frac{7\zeta(3)N_i}{16\pi^2(k_B T_{c0})^2}, \tag{12}$$

$$\gamma_i = \frac{7\zeta(3)\hbar^2 N_i v_{Fi}^2}{16\pi^2(k_B T_{c0})^2} \quad \text{and} \quad R_{12} = \frac{N_1\lambda_{12}}{\lambda} = \frac{N_2\lambda_{21}}{\lambda}. \tag{13}$$

Here, $\lambda_{ii'} = g_{ii'}N_{i'}$ with $N_{i'}$ the density of states at the Fermi level for each band, $\lambda = \lambda_{11}\lambda_{22} - \lambda_{12}\lambda_{21}$ and $\lambda_{\max} = \frac{1}{2}\left[(\lambda_{11} + \lambda_{22}) + \sqrt{(\lambda_{11} - \lambda_{22})^2 + 4\lambda_{12}\lambda_{21}}\right]$ are the determinant and the largest eigenvalue of λ-matrix, respectively. T_{c0} is the bulk critical temperature, and v_{Fi} is the average Fermi velocity for each band. $\boldsymbol{A}$ represents the vector potential.

In the spatially homogeneous case, we can neglect the gradient γ-terms. Equations (10) and (11) yield the gap equations at $T = T_{c0}$

$$\begin{pmatrix} \lambda_{11} & \lambda_{12} \\ \lambda_{21} & \lambda_{22} \end{pmatrix} \begin{pmatrix} \Delta_1 \\ \Delta_2 \end{pmatrix} = \lambda_{\max} \begin{pmatrix} \Delta_1 \\ \Delta_2 \end{pmatrix}, \tag{14}$$

which obviously give the consistent result.

From Eqs. (10) and (11), we can also read the weak-coupling two-band GL functional as

$$F_V = F_1 + F_2 + F_{12} \tag{15}$$

with

$$F_i = \int_V \left[\alpha_i(T)|\Delta_i|^2 + (\beta_i/2)|\Delta_i|^4 + \gamma_i|(\nabla - \mathrm{i}\boldsymbol{A})\Delta_i|^2\right] \mathrm{d}\boldsymbol{r} \tag{16}$$

and

$$F_{12} = \int_V (-R_{12}\Delta_1^*\Delta_2 + \text{c.c.})\mathrm{d}\boldsymbol{r}. \tag{17}$$

For a superconductor–insulator (or vacuum) interface, we can add new surface terms which take the form as

$$F_S = \int_S \left(\sum_{ii'} \gamma_i D_{ii'} \Delta_i^* \Delta_{i'} \right) d\boldsymbol{s} \tag{18}$$

with $D_{ii'}$ as the constant, and the integral runs over the surface of the superconductor.

Now, the total free energy is given by

$$F = F_V + F_S. \tag{19}$$

With the variation condition $\delta F/\delta\Delta_i^* = 0$, we can not only obtain the two-band GL equations (10) and (11), but also the boundary conditions

$$(\nabla - \mathrm{i}\boldsymbol{A})\Delta_i \cdot \boldsymbol{s}|_S = -\sum_{i'} D_{ii'}\Delta_{i'}. \tag{20}$$

In the absence of external magnetic field, we can set $\boldsymbol{A} = 0$ in Eq. (20). From Eq. (20), we can see that the ordinary Neumann boundary condition corresponds to $D_{ii'} = 0$. But we will find that the boundary effect induced by these D-terms is important for the understanding of the T_c suppression in MgB_2 thin films.

At this point, we would like to compare this boundary condition with that of the TDGL theory. In the GL theory, the effect of surface can be simply described by means of the boundary condition. First of all, from the general form of the self-consistent gap equation, we can find that only the odd powers of the gap function Δ will occur in the expansion at the boundary. Secondly, we also expect that nonlinear effects are small, and only the linear term is important in the GL region ($\Delta \ll k_B T_c$). Thirdly, higher derivatives of Δ will not exist in the boundary condition since these terms can be expressed in terms of the first and zeroth derivatives by the GL equation. Based on the discussion above, it is easy to justify that the boundary conditions

of TDGL and two-band GL theories will take the forms as $(\nabla - \mathrm{i}\boldsymbol{A})\Delta \cdot \boldsymbol{s}|_S = -\Delta/b$ with b the de Gennes surface extrapolation length and Eq. (20), respectively. The extra terms in the two-band GL theory are generated by the linear expansion of both Δ_1 and Δ_2. In principle, all the coefficients b and $D_{ii'}$ can be precisely determined by solving the linearized gap equations. And both boundary conditions assure the gauge invariance dictated by the basic structure of the GL theory.

Meanwhile, we would also like to point out that based on the two-gap theory, the boundary effect and different interband interactions in multi-band superconductors have already been extensively studied in the literature. With the Neumann boundary condition, the stable edge states and the dynamic response of such states to an external applied current have been investigated in the TDGL formalism for the mesoscopic superconductors [27–29]. Based on the tight-binding model and the free boundary condition, a microscopic study on the behavior of the order parameters near the boundaries has also been performed for multi-band superconducting materials [30]. With the Neumann boundary condition, Aguirre et al. discussed the effect of different interband interactions on the vortex states by solving the two-band TDGL equations [31–33]. However, to explain the suppression of critical temperature with the decrease in film thickness for MgB_2, we need to conduct the detailed microscopic analysis and derive the correct boundary terms within the two-band Bogoliubov–de Gennes theory for this superconductor.

3 The Microscopic Origin of Boundary Terms

Now, we examine the behavior of the superconducting order parameters near the superconductor–insulator interface based on the two-band Bogoliubov–de Gennes theory. In all cases, we assume that there is no current flowing through the boundary. We will show that the characteristic length scales of the boundary effect $D_{ii'}$ can be estimated by the linearized self-consistency equations in the neighborhood of the surface. The equation to be solved reads

$$\Delta_i(s) = \sum_{i'} \int K_{ii'}(s, s')\Delta_{i'}(s')\mathrm{d}s' \tag{21}$$

where s measures the normal distance from the boundary. For simplicity, we set the cross section of the boundary as 1. $K_{ii'}(s, s')$ is defined by Eq. (9) and due to the existence of the interface, $\Delta_i(s)$ will decrease exponentially in the insulating regime.

Following the procedure suggested by de Gennes [26], we suppose that the form of gap functions close to the surface behaves as

$$\Delta_i(s) = \Delta_{i0} + \left(\sum_{i'} D_{ii'}\Delta_{i'0} \right) s \tag{22}$$

with Δ_{i0} the gap function at the boundary and $s > 0$ inside the superconductor. It is easy to see that the boundary condition Eq. (20) follows naturally from Eq. (22). However, beyond the scale of the coherence length from the boundary, the linear

dependence definitely becomes invalid. Δ_i will then show a negative curvature and reach the BCS value deep in the superconductor.

If we introduce $K^0_{ii'}(s,s')$ as the kernel of gap functions in the bulk metal, we can then transform Eq. (21) as

$$\begin{aligned}&\Delta_i(s)-\sum_{i'}\int K^0_{ii'}(s,s')\Delta_{i'}(s')\mathrm{d}s'\\&=-\sum_{i'}\int[K^0_{ii'}(s,s')-K_{ii'}(s,s')]\Delta_{i'}(s')\mathrm{d}s'\equiv-\sum_{i'}H_{ii'}(s).\end{aligned}\tag{23}$$

From Eqs. (10) and (11) with the higher order β-terms omitted, also noting that $K^0_{ii'}(s,s')=K^0_{ii'}(s-s')$ due to the translational symmetry, we can read out the Laplace transformation of $K^0_{ii'}$ close to the critical temperature as

$$K^0_{ii'}(p)=\frac{\lambda_{ii'}}{\lambda_{\max}}+\frac{\lambda_{ii'}\gamma_{i'}}{N_{i'}}p^2.\tag{24}$$

Plugging Eqs. (24) into (23), we can get

$$\Delta_i(p)-\sum_{i'}\left(\lambda_{ii'}/\lambda_{\max}\right)\Delta_{i'}(p)-\sum_{i'}\left(\lambda_{ii'}\gamma_{i'}/N_{i'}\right)p^2\Delta_{i'}(p)=-\sum_{i'}H_{ii'}(p).\tag{25}$$

Here, $\Delta_i(p)$ and $H_{ii'}(p)$ are the Laplace transformations of $\Delta_i(s)$ and $H_{ii'}(s)$, respectively. Since the first two terms of the left-handed side in Eq. (25) can be approximately cancelled out according to Eq. (14), we then have

$$\sum_{i'}\left(\lambda_{ii'}\gamma_{i'}/N_{i'}\right)p^2\Delta_{i'}(p)=\sum_{i'}H_{ii'}(p).\tag{26}$$

We can see that both sides in Eq. (26) take the main contribution from the boundary region. Notice that the Laplace transformation of the gap functions in Eq. (22) takes the form

$$\Delta_i(p)=\frac{\Delta_{i0}}{p}+\sum_{i'}\frac{D_{ii'}\Delta_{i'0}}{p^2}.\tag{27}$$

Then at $p\to 0$, we will obtain from Eq. (26)

$$\sum_{i'i''}\left(\lambda_{ii'}\gamma_{i'}/N_{i'}\right)D_{i'i''}\Delta_{i''0}=\sum_{i'}H_{ii'}(p=0).\tag{28}$$

According to de Gennes' analysis [26, 34], from the sum rules

$$\int K^0_{ii'}(s,s')\mathrm{d}s'=\frac{\lambda_{ii'}}{\lambda_{\max}}\quad\text{and}\quad\int K_{ii'}(s,s')\mathrm{d}s'=\frac{\lambda_{ii'}N_{i'}(s)}{\lambda_{\max}N_{i'}}\tag{29}$$

with $N_{i'}(s)$ the local density of states at the Fermi surface, we can write the Laplace transformation of the kernel difference at $p\to 0$

$$H_{ii'}(p=0) = \int H_{ii'}(s)ds = \frac{\lambda_{ii'}\Delta_{i'0}}{\lambda_{\max}} \int \frac{\Delta_{i'}(s)}{\Delta_{i'0}} \left[1 - \frac{N_{i'}(s)}{N_{i'}}\right] ds. \tag{30}$$

$\Delta_{i'}(s)/\Delta_{i'0}$ approaches zero in the insulating region and is of the order of 1 in the metallic region. $N_{i'}(s)/N_{i'}$ also passes from $0 \to 1$ in a few interatomic distances from the boundary. Therefore, the integrand in Eq. (30) is nonvanishing only in a width of order of the lattice constant a. We can then estimate $H_{ii'}(p=0)$ as

$$H_{ii'}(p=0) = \frac{\lambda_{ii'}a}{\lambda_{\max}}\Delta_{i'0}. \tag{31}$$

Combining Eqs. (28) with (31), we can finally obtain

$$D_{ii} = \frac{N_i a}{\gamma_i \lambda_{\max}} \quad \text{and} \quad D_{12} = D_{21} = 0. \tag{32}$$

With these formulae, we successfully demonstrate the microscopic origin of the boundary conditions in Eq. (20).

At this stage, we would like to point out that $D_{ii'} = 0$ $(i \neq i')$ is only an approximation and will become nonzero in the higher-order calculation. Even for a contact between a superconductor and an insulator, the Cooper pairs can still diffuse into the insulating region with some probability. Algebraically, this means that the gap function $\Delta_{i'}(s)$ will also extend up to a distance of a into the $s < 0$ region, and from the self-consistent gap equations, we can qualitatively estimate $\Delta_{i'}(s) \sim \sum_{i''} T_{i'i''}\Delta_{i''0}e^{s/a}$ $(s < 0)$ with $T_{i'i''}$ the element of the transmission matrix at the boundary. Including the $s < 0$ part in the integration of Eq. (30) and noting $N_{i'}(s)/N_{i'} \approx 0$ in this region, we can get $H_{ii'}(p=0) = \frac{\lambda_{ii'}a}{\lambda_{\max}}(\Delta_{i'0} + \sum_{i''} T_{i'i''}\Delta_{i''0})$. Plugging into Eq. (28), the coefficients of boundary terms are given by

$$D_{ii} = \frac{N_i a}{\gamma_i \lambda_{\max}}(1 + T_{ii}), \quad D_{12} = \frac{N_1 a}{\gamma_1 \lambda_{\max}} T_{12} \quad \text{and} \quad D_{21} = \frac{N_2 a}{\gamma_2 \lambda_{\max}} T_{21}. \tag{33}$$

With the transmission coefficient from the superconductor to the insulator $T_{ii'} \ll 1$, we can obviously see that $D_{ii'} = 0$ $(i \neq i')$ is a good approximation.

4 Critical Temperature of MgB_2 Films in the Ginzburg–Landau Theory

In this section, we try to understand the film thickness dependence of T_c for MgB_2 based on the boundary effect mentioned above. We suppose that the film extends from $z = -d/2$ to $z = d/2$, and the film thickness is d.

From Eqs. (10) and (11), the two-band GL equations can be written as

$$\begin{pmatrix} \hat{H}_{11} & \hat{H}_{12} \\ \hat{H}_{21} & \hat{H}_{22} \end{pmatrix} \begin{pmatrix} \Delta_1(\boldsymbol{r}) \\ \Delta_2(\boldsymbol{r}) \end{pmatrix} = 0 \tag{34}$$

with

$$\hat{H}_{ii} = -\gamma_i \nabla^2 + \alpha_i(T) \tag{35}$$

and

$$\hat{H}_{12} = \hat{H}_{21} = -R_{12}. \tag{36}$$

Noting that close to the critical temperature, the magnitude of the order parameters is small and the higher-order β terms can be neglected.

Similar to the single-band case [34], we set the form of gap functions for the superconducting film as

$$\begin{pmatrix} \Delta_1(z) \\ \Delta_2(z) \end{pmatrix} = \begin{pmatrix} \mu_1 \cos(k_1 z) \\ \mu_2 \cos(k_2 z) \end{pmatrix} \tag{37}$$

with μ_i as the constant. Then from the boundary conditions

$$\left.\frac{\mathrm{d}\Delta_i}{\mathrm{d}z}\right|_{z=\pm d/2} = \mp D_{ii}\Delta_i, \tag{38}$$

we have k_i satisfying

$$k_i \tan\left(\frac{k_i d}{2}\right) = D_{ii}. \tag{39}$$

Let us introduce

$$H_{ii'} = \langle \Delta_i | \hat{H}_{ii'} | \Delta_{i'} \rangle = \int_{-d/2}^{d/2} \Delta_i(z) \hat{H}_{ii'} \Delta_{i'}(z) \mathrm{d}z, \tag{40}$$

we can transform Eq. (34) into

$$\begin{pmatrix} H_{11} & H_{12} \\ H_{21} & H_{22} \end{pmatrix} \begin{pmatrix} \mu_1 \\ \mu_2 \end{pmatrix} = 0 \tag{41}$$

with

$$H_{ii} = \left[\gamma_i k_i^2 + \alpha_i(T)\right] \left[\frac{d}{2} + \frac{\sin(k_i d)}{2k_i}\right] \tag{42}$$

and

$$H_{12} = H_{21} = -R_{12} \left[\frac{\sin\left(\frac{k_1 d}{2} + \frac{k_2 d}{2}\right)}{k_1 + k_2} + \frac{\sin\left(\frac{k_1 d}{2} - \frac{k_2 d}{2}\right)}{k_1 - k_2} \right]. \tag{43}$$

The critical temperature of the two-band superconducting film will be determined by the condition

$$H_{11}H_{22} - H_{12}H_{21} = 0 \tag{44}$$

at $T = T_c$, which can be explicitly written as

$$\prod_{i=1,2}\left[\gamma_i k_i^2 + \alpha_i(T_c)\right]\left[\frac{d}{2} + \frac{\sin(k_i d)}{2k_i}\right] = R_{12}^2\left[\frac{\sin(\frac{k_1 d}{2} + \frac{k_2 d}{2})}{k_1 + k_2} + \frac{\sin(\frac{k_1 d}{2} - \frac{k_2 d}{2})}{k_1 - k_2}\right]^2. \tag{45}$$

For the typical two-band superconductor MgB_2, we have $T_{c0} \approx 40$ K [35] and the average lattice constant $a \approx 0.4$ nm [36]. The density of states at the Fermi level for the σ band is $N_1 = 0.16$ eV^{-1}, and the value for the π band is $N_2 = 0.25$ eV^{-1} [4]. Since the theoretical fit to specific heat data gives $\lambda_{11} = g_{11}N_1 = 0.4$ and the ratio g_{11}:g_{22}:g_{12} = 1:0.3:0.2 [21], we can get $\lambda = 0.066$, $\lambda_{\max} = 0.44$ and $R_{12} = 0.30$ eV^{-1}. With the average Fermi velocities $v_{F1} = 3.7$ and $v_{F2} = 4.5$ in units of 10^{14} nm $\cdot$ s^{-1} from the numerical integration of the tight-binding calculations [4], we have $\gamma_1 = 39$ nm$^2 \cdot$ eV^{-1} and $\gamma_2 = 87$ nm$^2 \cdot$ eV^{-1} from Eq. (13). Then from Eq. (32), we can obtain the characteristic length scales $D_{11} = (268\ \text{nm})^{-1}$ and $D_{22} = (383\ \text{nm})^{-1}$. For a given film thickness d, we get k_i from Eq. (39). Plugging into Eq. (45), the critical temperature T_c as a function of d can be calculated numerically and then plotted in Fig. 1. It is shown that the critical temperature keeps gradually decreasing with the decrease in d and $T_c \approx 33$ K when the film thickness is reduced to $d = 10$ nm. From Fig. 1, we can see that our theoretical results fit the experimental data on different substrates very well.

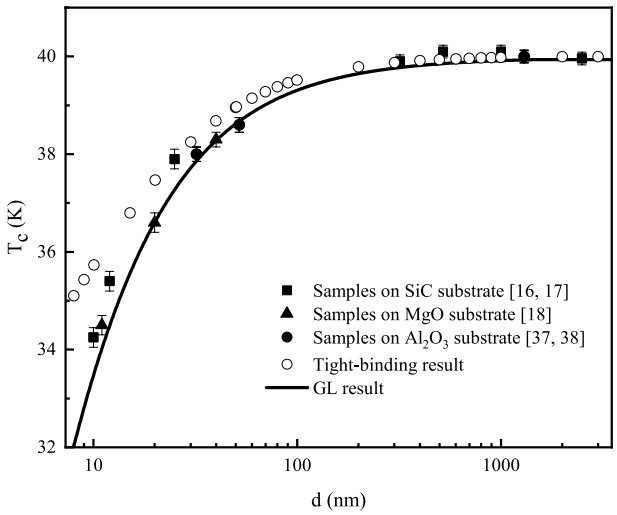

Fig. 1 Critical temperature as a function of the MgB_2 film thickness

5 Critical Temperature Calculations in the Tight-Binding Approximation

In this section, we present the calculation of gap functions and critical temperature for MgB_2 films based on the tight-binding model. The MgB_2 crystal consists of the subsequent, equally separated parallel honeycomb graphene-like layers of B and hexagonal planes of Mg atoms. Owing to this layered structure, the typical orientation of films is (0001), and we will limit ourselves to consider only such configuration. The z-direction is chosen perpendicular to the layer plane. As we know, the band structure calculations in the tight-binding approximation involve only boron electronic orbitals, so that only the boron atom positions inside the film are important. Let us label the subsequent boron layers as $\nu = 0, 1, \cdots, M$. Then, the total thickness of the MgB_2 film is $d = Ma$.

In the tight-binding model, the dispersion relations for σ and π bands are, respectively, given by

$$\varepsilon_{1\boldsymbol{k}} = e_1 - t_1 \cos(k_z a) - t_1'(k_x^2 + k_y^2)a^2 \tag{46}$$

and

$$\varepsilon_{2\boldsymbol{k}} = e_2 + t_2 \cos(k_z a) - t_2' \sqrt{1 + 4\cos\left(\frac{k_y a}{2}\right)\left[\cos\left(\frac{\sqrt{3}k_x a}{2}\right) + \cos\left(\frac{k_y a}{2}\right)\right]} \tag{47}$$

with $e_1 = 0.58$ eV, $t_1 = 0.19$ eV, $t_1' = 0.23$ eV, $e_2 = 0.04$ eV, $t_2 = 1.84$ eV, $t_2' = 1.60$ eV [4]. We assume an infinite quantum well for the electrons at the boundaries in the z-direction, and our construction of the trial electron wave functions follows the calculation of Szczeniowski and Wojtczak [39–42]. Then for this multi-layer system, we can rewrite the linearized gap equation in Eqs. (8) and (9) as

$$\Delta_i(\nu) = \sum_{i',\nu'} K_{ii'}(\nu, \nu')\Delta_{i'}(\nu') \tag{48}$$

with

$$K_{ii'}(\nu, \nu') = \frac{g_{ii'}}{2} \sum_{\boldsymbol{k}\boldsymbol{k}'} \frac{\tanh\left(\frac{\varepsilon_{i'\boldsymbol{k}}}{2k_BT}\right) + \tanh\left(\frac{\varepsilon_{i'\boldsymbol{k}'}}{2k_BT}\right)}{\varepsilon_{i'\boldsymbol{k}} + \varepsilon_{i'\boldsymbol{k}'}} \Gamma_{k_z}^*(\nu')\Gamma_{k_z'}^*(\nu')\Gamma_{k_z}(\nu)\Gamma_{k_z'}(\nu). \tag{49}$$

Noting here that the factor $\exp(\mathrm{i}\nu k_z a)$ satisfying the Bloch condition in the z-direction for the bulk crystal is replaced by the more general amplitude

$$\Gamma_{k_z}(\nu) = \frac{\sin(\nu k_z a)}{\sqrt{\sum_{\nu=0}^{M} \sin^2(\nu k_z a)}} \tag{50}$$

and $k_z = \frac{m\pi}{d}$ $(m = 0, 1, \cdots, M)$ is the discrete wave vector allowed in the infinite potential well.

We perform the numerical calculations for the films composed of $20 \sim 10000$ boron layers, corresponding to a film thickness roughly $8 \sim 4000$ nm. For a given temperature, we compute the kernel $K_{ii'}(\nu, \nu')$ first. We use the Monte Carlo technique to do the summation on k_x and k_y, and a number of 10^8 random wave vectors (k_x,k_y) are generated from the two-dimensional first Brillouin zone. The energy cutoff for $\varepsilon_{i'\boldsymbol{k}}$ and $\varepsilon_{i'k'}$ is taken as $k_B\Theta_D$ with Θ_D the Debye temperature. To fit the critical temperature for the bulk system, we choose $\Theta_D = 750$ K [36]. We then iteratively compute the gap function $\Delta_i(\nu)$ from Eq. (48) with the initial value setting as 10 meV. The convergence criterion we adopt is $|\Delta_i^{n+1}(\nu) - \Delta_i^n(\nu)|/\Delta_i^n(\nu) \leqslant 10^{-8}$, where n numbers the iteration. Finally, T_c is determined by the maximum temperature with the existence of a nonzero solution of $\Delta_i(\nu)$ in the layered system. The calculated critical temperature as a function of the film thickness d is also presented in Fig. 1. It is shown that the critical temperature keeps decreasing with the decrease in d and T_c drops to about 36 K at $d = 10$ nm which is 9% greater than the GL result. From Fig. 1, we can see that the tight-binding calculations are qualitatively consistent with the experimental data and the GL theory.

6 Conclusion

In conclusion, we introduce the appropriate boundary conditions in the two-band GL theory at the interface between a two-gap superconductor and an insulator (or vacuum). We also give a microscopic derivation of these boundary terms based on the two-band Bogoliubov–de Gennes formalism. For the typical two-band superconductor MgB_2, we obtain the characteristic length scales of the boundary effect as 268 and 383 nm. It can perfectly explain the dramatic suppression of T_c when the film thickness is reduced to the same order of these scales. Our investigation thus suggests that the boundary effect induced by these new terms may play an important role in the research of multi-band superconducting films.

Declarations

Conflict of interest The authors declare that they have no conflict of interest.

Informed consent Informed consent was obtained from all individual participants included in the study.

References

1. J. Nagamatsu, N. Nakagawa, T. Muranaka, Y. Zenitani, J. Akimitsu, Nature **410**, 63 (2001). https://doi.org/10.1038/35065039
2. J. Kortus, I.I. Mazin, K.D. Belashchenko, V.P. Antropov, L.L. Boyer, Phys. Rev. Lett. **86**, 4656 (2001). https://doi.org/10.1103/PhysRevLett.86.4656
3. J.M. An, W.E. Pickett, Phys. Rev. Lett. **86**, 4366 (2001). https://doi.org/10.1103/PhysRevLett.86.4366
4. Y. Kong, O.V. Dolgov, O. Jepsen, O.K. Andersen, Phys. Rev. B **64**, 020501(R) (2001). https://doi.org/10.1103/PhysRevB.64.020501

5. K.P. Bohnen, R. Heid, B. Renker, Phys. Rev. Lett. **86**, 5771 (2001). https://doi.org/10.1103/PhysRevLett.86.5771
6. A.Y. Liu, I.I. Mazin, J. Kortus, Phys. Rev. Lett. **87**, 087005 (2001). https://doi.org/10.1103/PhysRevLett.87.087005
7. A. Brinkman, A.A. Golubov, H. Rogalla, O.V. Dolgov, J. Kortus, Y. Kong, O. Jepsen, O.K. Andersen, Phys. Rev. B **65**, 180517(R) (2002). https://doi.org/10.1103/PhysRevB.65.180517
8. F. Giubileo, D. Roditchev, W. Sacks, R. Lamy, D.X. Thanh, J. Klein, S. Miraglia, D. Fruchart, J. Marcus, P. Monod, Phys. Rev. Lett. **87**, 177008 (2001). https://doi.org/10.1103/PhysRevLett.87.177008
9. P. Szabó, P. Samuely, J. Kačmarčík, T. Klein, J. Marcus, D. Fruchart, S. Miraglia, C. Marcenat, A.G.M. Jansen, Phys. Rev. Lett. **87**, 137005 (2001). https://doi.org/10.1103/PhysRevLett.87.137005
10. F. Bouquet, R.A. Fisher, N.E. Phillips, D.G. Hinks, J.D. Jorgensen, Phys. Rev. Lett. **87**, 047001 (2001). https://doi.org/10.1103/PhysRevLett.87.047001
11. I.I. Mazin, J. Kortus, Phys. Rev. B **65**, 180510(R) (2002). https://doi.org/10.1103/PhysRevB.65.180510
12. Y. Bugoslavsky, Y. Miyoshi, G.K. Perkins, A.V. Berenov, Z. Lockman, J.L. MacManus-Driscoll, L.F. Cohen, A.D. Caplin, H.Y. Zhai, M.P. Paranthaman, H.M. Christen, M. Blamire, Supercond. Sci. Technol. **15**, 526 (2002). https://doi.org/10.1088/0953-2048/15/4/308
13. X.X. Xi, A.V. Pogrebnyakov, X.H. Zeng, J.M. Redwing, S.Y. Xu, Q. Li, Z.K. Liu, J. Lettieri, V. Vaithyanathan, D.G. Schlom, H.M. Christen, H.Y. Zhai, A. Goyal, Supercond. Sci. Technol. **17**, S196 (2004). https://doi.org/10.1088/0953-2048/17/5/021
14. X.H. Zeng, A.V. Pogrebnyakov, A. Kotcharov, J.E. Jones, X.X. Xi, E.M. Lysczek, J.M. Redwing, S.Y. Xu, Q. Li, J. Lettieri, D.G. Schlom, W. Tian, X.Q. Pan, Z.K. Liu, Nat. Mater. **1**, 35 (2002). https://doi.org/10.1038/nmat703
15. X.X. Xi, X.H. Zeng, A.V. Pogrebnyakov, S.Y. Xu, Q. Li, Y. Zhong, C.O. Brubaker, Z.K. Liu, E.M. Lysczek, J.M. Redwing, J. Lettieri, D.G. Schlom, W. Tian, X.Q. Pan, IEEE Trans. Appl. Supercond. **13**, 3233 (2003). https://doi.org/10.1109/TASC.2003.812209
16. Y.L. Chen, C. Yang, C.Y. Jia, Q.R. Feng, Z.Z. Gan, Physica C **525–526**, 56 (2016). https://doi.org/10.1016/j.physc.2016.02.022
17. C. Zhang, Y. Wang, D. Wang, Y. Zhang, Z.H. Liu, Q.R. Feng, Z.Z. Gan, J. Appl. Phys. **114**, 023903 (2013). https://doi.org/10.1063/1.4812738
18. J.Y. Pan, C. Zhang, F. He, Q.R. Feng, Acta Phys. Sin. **62**, 127401 (2013). https://doi.org/10.7498/aps.62.127401
19. M.P.A. Fisher, G. Grinstein, S.M. Girvin, Phys. Rev. Lett. **64**, 587 (1990). https://doi.org/10.1103/PhysRevLett.64.587
20. A.M. Finkel'stein, Phys. B **197**, 636 (1994). https://doi.org/10.1016/0921-4526(94)90267-4
21. M.E. Zhitomirsky, V.H. Dao, Phys. Rev. B **69**, 054508 (2004). https://doi.org/10.1103/PhysRevB.69.054508
22. L.F. Zhang, L. Covaci, M.V. Milošević, G.R. Berdiyorov, F.M. Peeters, Phys. Rev. Lett. **109**, 107001 (2012). https://doi.org/10.1103/PhysRevLett.109.107001
23. L.F. Zhang, L. Covaci, M.V. Milošević, G.R. Berdiyorov, F.M. Peeters, Phys. Rev. B **88**, 144501 (2013). https://doi.org/10.1103/PhysRevB.88.144501
24. L.F. Zhang, V.F. Becerra, L. Covaci, M.V. Milošević, Phys. Rev. B **94**, 024520 (2016). https://doi.org/10.1103/PhysRevB.94.024520
25. L.F. Zhang, L. Covaci, M.V. Milošević, Phys. Rev. B **96**, 224512 (2017). https://doi.org/10.1103/PhysRevB.96.224512
26. P.G. de Gennes, *Superconductivity of Metals and Alloys* (Westview Press, New York, 1966). https://doi.org/10.1201/9780429497032
27. W.C. Gonçalves, E. Sardella, V.F. Becerra, M.V. Milošević, F.M. Peeters, J. Math. Phys. **55**, 041501 (2014). https://doi.org/10.1063/1.4870874
28. V.F. Becerra, M.V. Milošević, Phys. Rev. B **94**, 184517 (2016). https://doi.org/10.1103/PhysRevB.94.184517
29. V.F. Becerra, M.V. Milošević, Physica C **533**, 91 (2017). https://doi.org/10.1016/j.physc.2016.07.002
30. A. Benfenati, A. Samoilenka, E. Babaev, Phys. Rev. B **103**, 144512 (2021). https://doi.org/10.1103/PhysRevB.103.144512
31. T.N. Jorge, C. Aguirre, A. de Arruda, J. Barba-Ortega, Eur. Phys. J. B **93**, 69 (2020). https://doi.org/10.1140/epjb/e2020-100418-4

32. C.A. Aguirre, Q.D. Martins, J. Barba-Ortega, Physica C **581**, 1353818 (2021). https://doi.org/10.1016/j.physc.2021.1353818
33. C. Aguirre, A.S. de Arruda, J. Faúndez, J. Barba-Ortega, Phys. B **615**, 413032 (2021). https://doi.org/10.1016/j.physb.2021.413032
34. J.B. Ketterson, S.N. Song, *Superconductivity* (Cambridge University Press, Cambridge, 1999). https://doi.org/10.1017/CBO9781139171090.011
35. X.X. Xi, Rep. Prog. Phys. **71**, 116501 (2008). https://doi.org/10.1088/0034-4885/71/11/116501
36. S.L. Bud'ko, G. Lapertot, C. Petrovic, C.E. Cunningham, N. Anderson, P.C. Canfield, Phys. Rev. Lett. **86**, 1877 (2001). https://doi.org/10.1103/PhysRevLett.86.1877
37. K.C. Zhang, L.L. Ding, C.G. Zhuang, L.P. Chen, C.P. Chen, Q.R. Feng, Phys. Status Solidi **203**, 2463 (2006). https://doi.org/10.1002/PSSA.200522262
38. X.J. Wang, C. Zhang, Y. Zhang, Q.R. Feng, Y. Wang, Chin. J. Low Temp. Phys. **38**, 64 (2016). https://doi.org/10.13380/j.cnki.chin.j.lowtemp.phys.2016.04.012
39. S. Szczeniowski, L. Wojtczak, Acta Phys. Pol. **36**, 241 (1969)
40. P. Czoschke, H. Hong, L. Basile, T.C. Chiang, Phys. Rev. Lett. **91**, 226801 (2003). https://doi.org/10.1103/PhysRevLett.91.226801
41. P. Czoschke, H. Hong, L. Basile, T.C. Chiang, Phys. Rev. B **72**, 035305 (2005). https://doi.org/10.1103/PhysRevB.72.035305
42. P. Czoschke, H. Hong, L. Basile, T.C. Chiang, Phys. Rev. B **72**, 075402 (2005). https://doi.org/10.1103/PhysRevB.72.075402